Potential Causes of Failure in an Aluminum Sand-Cast Pot from Zambia

Alec Radford, Janie Harari, Steph Northway, and Ben Kroop

Fig. 1. The Zambian pot being analyzed.

***Abstract*—An investigation into the failure of sand cast aluminum pots was conducted. These pots were made with with recycled aluminum by a small business in Zambia. The most common failure mode of these pots is the legs breaking off in a brittle manner. Three possible causes of failure were explored: impurities (particularly iron) in the microstructure, gas porosity caused by poor casting methods, and the geometry of the pot. Based off EDS and SEM results, tensile testing on cast dogbones, and SolidWorks finite element analysis, the geometry of the pot is the most likely cause of this problem.**

I. Introduction and Overview

IN the last few years, Zambia has experienced sustained economic growth and a growing demand for consumer goods, including those made of aluminum [1]. As a result, the price of professionally smelted aluminum has increased significantly in Zambia. Many small scale operations have turned to sourcing their own scrap aluminum for recycling into new products. Though recycled aluminum coupled with chemical free sand casting is an environmentally benign process when compared to the alternatives, there have been reports that this transition has resulted in a noticeable increase in brittleness in the pot. The home-sourced scrap has resulted in metals besides aluminum being included in the melt, which could possibly be the source of this problem [2]. Specifically, one product, a sand cast aluminum pot, now often breaks when dropped whereas before there were very few reported problems with it.

As a first area of investigation, the effects of uncontrolled impurities being introduced into the casting process were explored through a variety of techniques including compositional analysis, microstructure analysis, and comparative experiments assessing the impacts of specific impurities on mechanical properties. Once the effects of impurities were well characterized, it was determined that they alone could not sufficiently explain the failure of the pot when dropped. As a result, further analysis to identify other sources of failure was conducted. This included the possibility of casting defects, such as gas porosity, and the mechanical design causing stress concentrations near areas of known failure. These results, combined with the historical narrative of the pot, identify the most likely source of failure. The mechanical design of the pot was originally developed with cast iron as the chosen material and switching to cast aluminum, a significantly weaker material, could have possibility resulted in a decrease in tolerances to the point where the pot was no longer able to withstand stresses encountered in everyday situations such as being dropped from carrying height. A modification of the mechanical design of the pot's legs is proposed which should provide sufficient tolerance to stresses encountered in everyday use - allowing for the continued use of cast aluminum.

II. Preliminary Microstructural Analysis

To determine the composition and microstructure of the pot's material, a half inch cylindrical sample was removed from the end of one of the pot's legs. To prepare the sample for imaging it was embedded in a plastic disk to provide a smooth, stable surface to mount to the SEM's stage. The mounted sample was then sanded and polished.

Before imaging the sample in the SEM, an optical microscope was used to determine areas and features of interest. A marking was drawn on the sample using a diamond-tipped engraving pen. Optical images were captured of the sample near the marking.

The sample was then placed in the scanning electron microscope, and the stage was moved until the marking was in frame. Because some features were less visible on the SEM than the optical microscope, the two images were compared, using the marking as a reference to the positions of features.

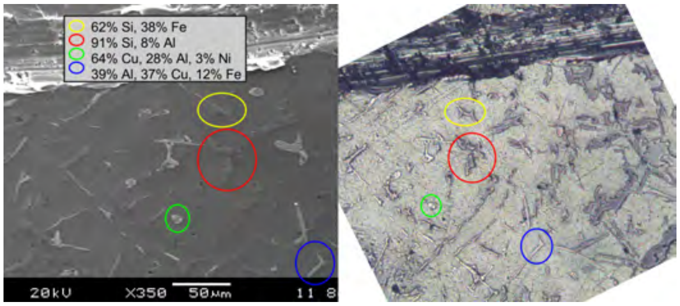

Fig. 2. The Zambian pot under the SEM (left) and optical (right) microscopes. Circled areas highlight specific elements of the microstructure.

To determine the composition of the overall sample, as well as specific features of the sample, the EDS was used in "point and shoot mode". This mode provides a list of elements present within at a point of interest, and exports the approximate percentage present.

The brighter, rounder features that were seen under the SEM (Figure 2) are mainly copper containing; the needle-like structures are iron containing, and the darker features are largely silicon. Copper is generally considered a strengthening element in aluminum alloys, but silicon and iron both have the potential to significantly reduce ductility if they are in high enough concentration. The EDS was not very reliable in determining overall concentrations in a sample (this was confirmed when it gave the wrong concentrations for an alloy of known composition), so the results that were obtained could not rule out the possibility that imputities were causing the pot to experience brittle fracture.

While silicon would have to be at a concentration greater than 12% to weaken the alloy, iron needles could provide an easy path for crack propagation in much smaller concentrations. Additionally, recycled aluminum is more likely to have excess iron than excess silicon; as only a small amount of iron would have to be present. Thus, iron content was chosen as the first potential cause of failure to investigate.

III. Method - Sand Casting

In an attempt to determine whether the brittleness of the pot was due to the composition of the Al alloy, multiple dog bones were sand cast using different Al alloys. Sand casting was chosen over other casting methods to replicate the process used to manufacture the pot in Zambia. Two sets of dog bones were cast. One set used the industrial Al-Si alloy A356, and the other used the same alloy with 0.02% iron by weight added to simulate the iron contamination in the scrap metal used to manufacture the pot in Zambia. Iron was introduced into the sample by measuring out the specified amount of iron powder and mixing it into the melt during casting.

A sand casting flask was used to create the two-part mold for the dog bones. Sand was mixed with bentonite clay powder and water to create a sticky, densely packed material for the mold. On one side of the mold, the sand mixture was pressed around nylon sample dog bones, then the nylon dog bones were removed to create -shaped cavities. On the other side of the mold, the sand mixture was pressed around a set of wax conical sprues and cylindrical sprues. The sprues were carefully aligned to create passages for the liquid metal to enter the on the first half of the mold, and to create vents for air in the mold to escape.

Fig. 3. The mold and sand cast dog bones

To cast the dog bones the two sides of the mold were brought together and the Al-Si was heated in an induction furnace. The molten aluminum was then poured into the molds. The two halves of the molds were separated after thirty seconds, the metal was allowed to air cool to room temperature, and the dog bones were removed from the mold by hand. This process was then repeated with Al-Si-Fe. It should be noted that the sand mold was destroyed and remade between castings.

IV. Results - Sand Casting

Instron tensile testing of the dog bones revealed that the pot's susceptibility to brittle fracture may be influenced by casting defects. This conclusion was drawn from the large variation that was seen in the samples that were tested. The stress at the yield point ranged from 115-127 MPa and the strain ranged from 3.1 mm/mm to 5.8 mm/mm for the dog bones with no iron impurities. The stress at the yield point ranged from 85 to 100 MPa and the strain ranged from 1.9 mm/mm to 5.3 mm/mm for the for the dog bones with iron impurities. The results of the testing from the four specimens, two of aluminum silicon and two of aluminum silicon with added iron, can be seen in Figure 8. Since the techniques that were used were not as refined as those used by people in Zambia who make sand cast products for a living, the observed defects may not be representative of all sand cast products but rather the skill of the casters.

The hypothesis being tested was that an iron weight concentration of .02% would cause the alloy to become observably less ductile. This hypothesis was based on the fact that the pot's composition was believed to be in the hypoeutectic region. However, after further research, it was found that most aluminum alloys contain iron impurities, with an average of 0.07% to 0.10% iron. This explains why no significant differences were found between the samples [3]. The wide variation between the stress-stain curves made it impossible to

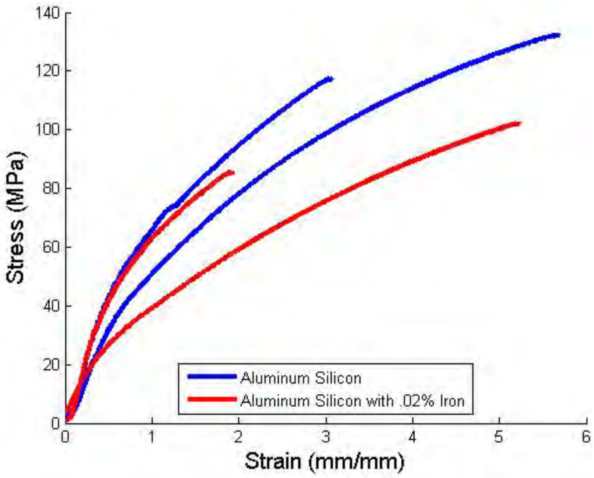

Fig. 4. Stress strain curves for the sand cast dog bones

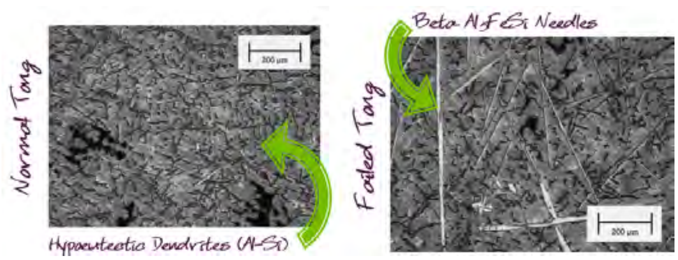

Fig. 5. Comparison of the normal and failed tongs from [8]. The iron content of the failed tong was much higher than that of the normal tong.

draw a conclusion that the iron was affecting the mechanical properties of recycled aluminum, nor was it enough to discount this theory.

V. Secondary Microstructural Analysis

Though the first investigation of iron content in sand-cast aluminum dog bones was inconclusive, by comparing the SEM and optical microscope photos to previous research [8] on the effect of iron in aluminum alloys in a pair of failed tongs, it was observed that the iron content was a less likely potential root cause of failure than first thought. The pot leg looks more similar to the normal tong than it does to the failed tong (Figure 5); there are no Al-Si-Fe needle/platelet structures greater than about 150 μm length in the pot sample (Figure 2), whereas the needles in the failed tong were thick and almost all greater than 400 μm in length. However, it was decided that the iron content was still worth investigating because there are no other obvious ways in which the impurities would contribute to brittle fracture.

From 0-.05% Fe (blue line), the alloy is in the alpha phase, where the iron is fully dissolved in the aluminum. This was the region where it was hypothesized that the alloy of the pot was when the sand cast dog bone samples were made. It was later discovered that this is also the region that the stock

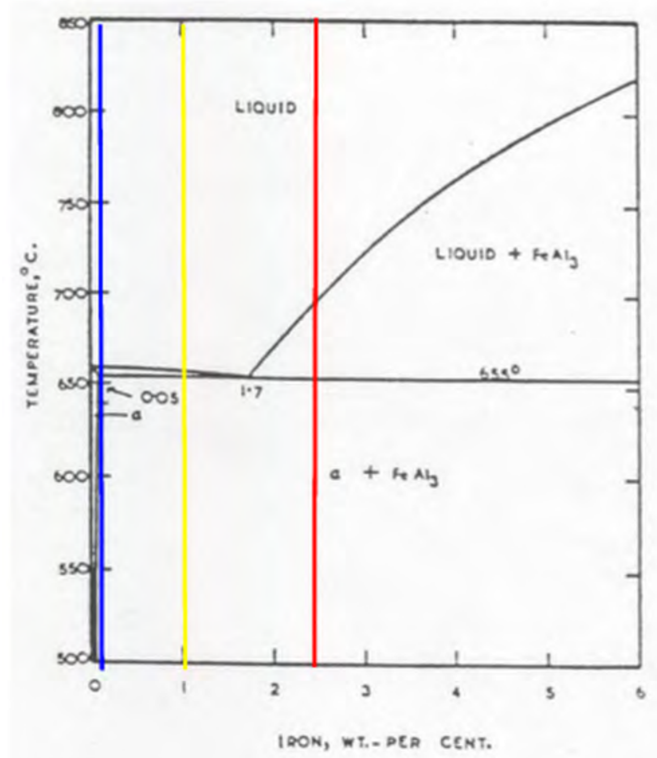

Fig. 6. The relevant part of the Al-Fe phase diagram, with some important regions highlighted. [9]

aluminum (alloy A356) lies in, since even molten primary aluminum contains on average 0.07% to 0.10% iron. [10] The results from the failed tongs demonstrate that the ductility of an iron-aluminum alloy was significantly reduced in the hypereutectic region including more than 1.7% iron. Based on the EDS results, the sample that was taken from the pot leg probably had less than 1% iron (yellow line), but more than the alpha phase (blue line) since the EDS did not pick up any traces, but there were clearly iron inclusions. Since the failed tongs were constructed from an alloy was in the hypereutectic phase, and the sample from the pot is most likely in the hypoeutectic phase, it is possible that hypoeutectic iron concentrations may not cause the alloy to become more susceptible to brittle fracture.

VI. Method - Lost Wax Casting

Because casting defects in the sand cast dog bones caused unreliable test results, and because the percentage of iron included in the sand-cast dog bones was lower than it should have been to test our hypothesis, three new sets of dog bones were cast using a wax investment casting. The first set of dog bones was cast out of the industrial Al-Si alloy A356. The second two sets of dog bones were cast out of the same alloy, but with 1% and 3% iron added by weight. These percentages represent the hypoeutectic and hypereutectic aluminum iron alloys, respectively. As in sand casting, iron was introduced into the sample by measuring out the appropriate amount of iron powder and mixing it into the melt before casting.

A separate mold was made for each of the three alloys. To create the mold, a conical wax sprue was attached to a rubber flask ring to stabilize it on a workbench. Acrylic dog bones were attached with hot sticky wax to 1mm diameter cylinders of wax to create dog bones on branches. The branches were then attached to the conical sprue using sticky wax to create a wax tree with acrylic dog bone leaves. A perforated casting flask was placed over the wax tree, then shrink-wrapped to seal the perforations and allow for the addition of the investment material.

For each mold, investment material powder was weighed and mixed with water in a bowl using an electric hand mixer until viscous and smooth. The wet investment material was placed under a vacuum to remove air trapped in the mixture. Immediately after removing the air from the mixture, the mold material was poured into the casting flask to form a negative around the tree.

The flasks were heat cycled overnight in an oven according to the investment material instructions to solidify the mold and melt the wax and acrylic that made up the tree inside out of the mold. With the molds still in the heated oven, aluminum was melted in an induction furnace. As the aluminum melted, iron powder was added, then stirred in vigorously with a graphite stick. The pre-heated mold was removed from the oven, and placed in a vacuum chamber such that the mold intake was open at the top, and the flask's perforations were inside the vacuum chamber. The vacuum was turned on, then the molten metal was poured into the mold. Before the metal solidified, the vacuum helped draw the metal into the extremities of the mold.

Once the excess metal on top of the mold had visibly solidified, the mold was submerged in a bucket of water to complete the cooling process and to soak off the investment material. Once the metal had cooled, the tree was removed from the water. The dog bones were removed from the tree and excess material was removed from each in a machine shop.

VII. Results - Lost Wax Casting

Instron tensile testing of the wax cast dog bones yielded two main results as per Figure 7. Since one of the samples was in the hypoeutectic region and the other was in the hypereutectic region, it was hypothesized that there would be an increase in brittleness. Using a T-test with an independent sampling assumption results in a p-value of 0.158 or near statistical significance comparing the distributions of hypoeutectic and hypereutectic Al-Fe alloys which is impressive for such a small sample size of 12 dog bones. Casting defects related to gas porosity resulted in high variance outliers. This conclusion was drawn from the relatively small cross-sectional area with relatively large bubbles along the fracture surfaces of the dog bones.

The maximal elongation for each set of dog bones was in the range of .3 mm/mm to 5.5 mm/mm and the yield strength for each set of dog bones was in the range of 75 MPa to 110 MPa, which is significantly lower than the expected yield strength of A356 and it's derivatives, which provides further evidence for the impact of casting defects on the results (Figure 8).

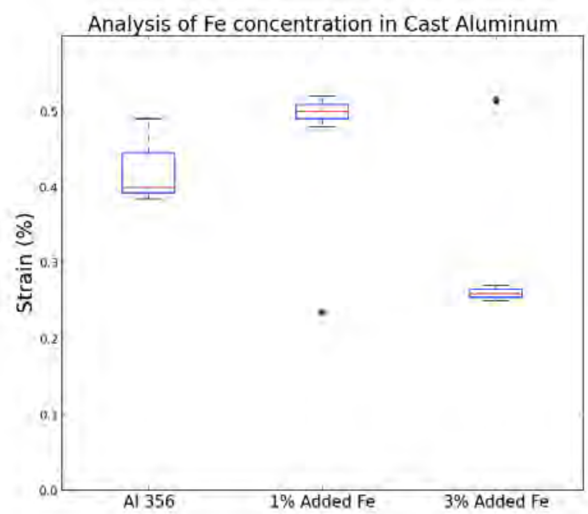

Fig. 7. Box and whisker plot of the maximal elongations of the lost wax cast dog bones. The outliers noted in red and are likely due to casting defects.

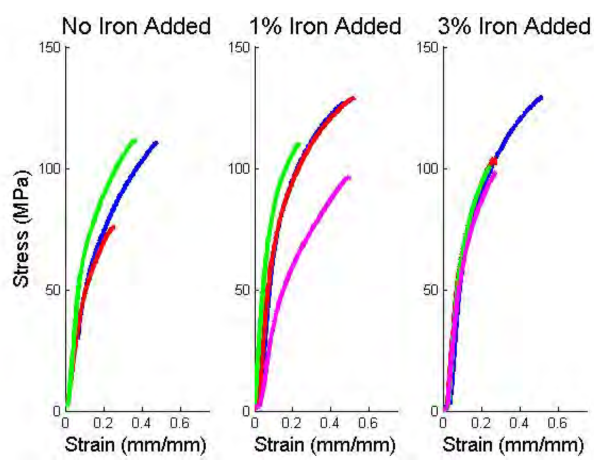

Fig. 8. Stress strain curves for the wax cast dog bones of A356, A356 with 1% added iron and A356 with 3% added iron

VIII. Professional Compositional Analysis

The pot and stock aluminum samples were subjected to EDS analysis several times, but because the concentration of Si was abnormally high and Fe was abnormally low, the samples were sent to Metallurgical Engineering Services Incorporated for professional compositional analysis. The results are pictured in Figures 9 and 10.

The pot sample has far fewer impurities than expected for recycled aluminum, and nearly matches industrial alloy A03320. Alloys A356 and A03320 fall into the same area of the ternary phase diagram for Al-Si-Fe as shown in Figure 11.

Element, Wt.%	A - Stock Cast Aluminum	UNS A03560
Silicon	6.38	6.5-7.5
Iron	0.18	0.6 max
Copper	0.08	0.25 max
Magnesium	0.32	0.35 max
Zinc	0.10	0.35 max
Titanium	0.11	0.25 max
Manganese	0.052	Each 0.05 max, Total 0.15 max **Note:** if Fe exceeds 0.45, Mn shall not be less than 0.5xFe
Chromium	0.030	
Nickel	0.030	
Boron	0.0002	
Beryllium	0.00004	
Bismuth	0.001	
Calcium	0.007	
Gallium	0.010	
Lithium	0.004	
Sodium	0.005	
Phosphorus	<0.001	
Lead	0.006	
Antimony	<0.0004	
Tin	0.001	
Strontium	0.003	
Vanadium	0.010	
Zirconium	0.002	
Aluminum	Remainder	Remainder

Fig. 9. Lab results for composition of stock aluminum.

Element, Wt.%	B - Zambian Pot	UNS A03320
Silicon	8.85	8.5-10.5
Iron	0.82	1.2 max
Copper	2.02	2.0-4.0
Manganese	0.19	0.50 max
Magnesium	0.30	0.50-1.5
Nickel	0.09	0.50 max
Zinc	0.67	1.0 max
Titanium	0.03	0.25 max
Chromium	0.043	Total 0.50 max
Boron	0.001	
Beryllium	0.0001	
Bismuth	0.0004	
Calcium	0.001	
Gallium	0.014	
Lithium	<0.0001	
Sodium	0.001	
Phosphorus	<0.001	
Lead	0.066	
Antimony	<0.0004	
Tin	0.018	
Strontium	<0.0001	
Vanadium	0.006	
Zirconium	0.003	
Aluminum	Remainder	Remainder

Fig. 10. Lab results for composition of the aluminum in the Zambian pot.

At 600°C, the phases present in both alloys include liquid and τ_6 ($Al_{4.5}SiFe$), also known as the beta phase. The stock aluminum sample also contains a primary aluminum (Al) phase, while the pot sample falls approximately on the line between the L + τ_6 + (Al) phase and the L + τ_6. This could explain the apparent absence of (Al) in the images of the pot sample.

Though the two samples (Figures 12 and 13) look very different because of the lack of (Al) phase in the pot, they are quite similar in composition. With the professional analysis of composition showing the pot sample to be in the acceptable ranges of all impurities and the results of testing on casted dog bones, it was finally concluded that iron content is most likely not the underlying cause of failure.

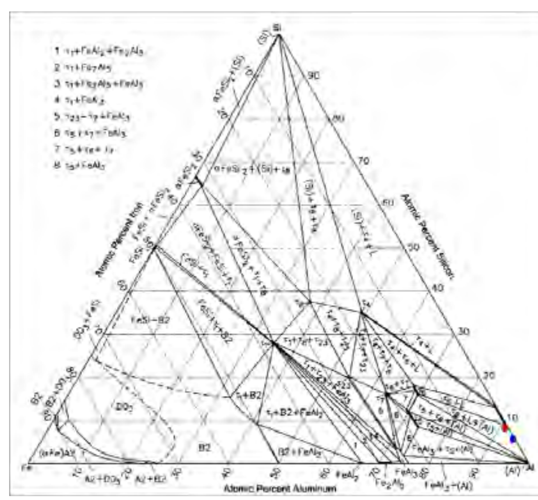

Fig. 11. Al-Si-Fe phase diagram at 600°C. Alloy A356 is represented by the blue dot, and A03320 is represented by the red. Modified from [4].

IX. Casting Defects - Gas Porosity

The observation of high variance outliers during the lost wax casting analysis demonstrates another potential source of failure in the pot - macrostructure casting defects caused primarily by gas porosity. Although manual inspection of a cross-section of a leg of the pot showed few defects, a significant amount of bubbles were observed on the fracture surface of the casting sprue. This indicates a high variance in the distribution of casting defects in the pot. In order to determine whether these defects could be a potential source of failure, an equation containing the fracture toughness, K_{ic} of

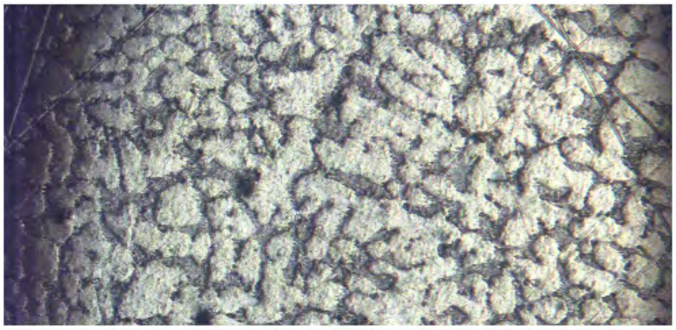

Fig. 12. The commerical Al-Si alloy at 200x magnification.

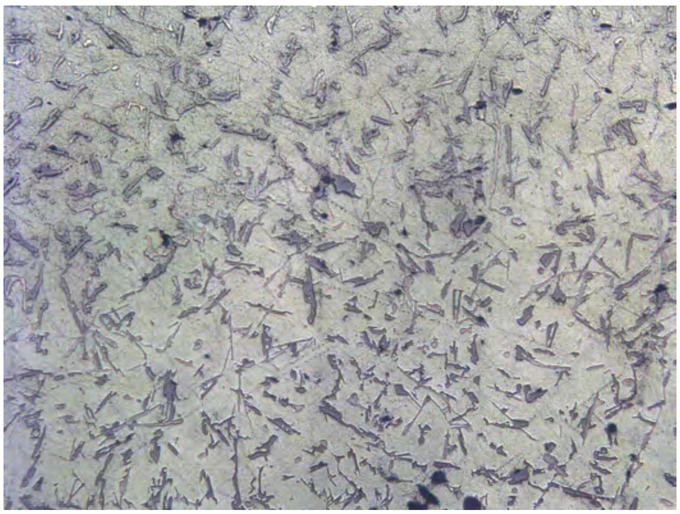

Fig. 13. The Zambian pot under the optical microscope at 200x magnification.

the pot alloy, a known critical stress of the most similar alloy as determined by the composition test was used to calculate the critical stress at which a fracture will occur due to defects.

$$K_{ic} = Y\sigma\sqrt{\pi a} \tag{1}$$

Solving for σ, the critical stress, results in the equation,

$$\sigma = \frac{K_{ic}}{Y\sqrt{\pi a}} \tag{2}$$

Using the radius of the largest observed defect, $\approx$0.7 mm, a constant value for Y around 1 (related to the geometry of the defect), and a fracture toughness of 18-23 $MPa\sqrt{m}$ results in a critical stress for failure due to casting defects of around 383-490 MPa. Since this value is well above the yield strength of the Al alloy, 192 MPa [12], casting defects are an unlikely source of failure.

X. Structural Analysis

Finite element analysis in SolidWorks was conducted to determine if the failure of the pot was due to its mechanical structure. To begin, conservation of energy equations were used to find the velocity right before impact

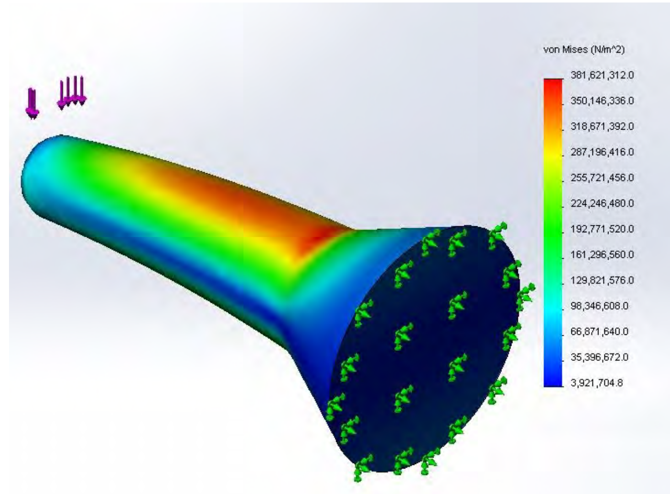

Fig. 14. The yield strength suggests that when this pot is made out of aluminum, it will fracture when dropped onto the leg in this orientation. The maximum stress experienced here is 384 MPa, and the yield strength of our aluminum alloy is 192 MPa [12]. For grey cast iron the yield strength is not defined, since the material is so brittle and the yield varies widely. [13]. However, the yield strength for malleable and ductile cast iron ranges from 224 MPa-864 MPa [14]. If the pot had been made out of this material instead, it probably would not have fractured.

$$mgh = \frac{1}{2}mv^2 \tag{3}$$

$$v = \sqrt{2gh} \tag{4}$$

Next, an equation relating the impulse of a force and the change in momentum was used to find a final value for the force.

$$F = \frac{mv}{t} = \frac{m\sqrt{2gh}}{t} \tag{5}$$

For a drop height of 4 m, the mass of the pot, which was found to be 2.84 kg, and a stopping time of 3 ms, it was found that the final force on the pot was 4590 N.

A model of the leg was created in SolidWorks, since that was the most likely fracture surface. It is important to note that although this is a dynamic force that the pot is experiencing, when the analysis was performed in SolidWorks, it was modeled as a static force. Through online research of a branding on the lid of the pot, it was found that the pot was originally made from cast iron. [11] The design decision to change the material of this pot from cast iron to cast aluminum drastically decreases the yield strength, making it much more susceptible to fracture when dropped. The result of this analysis is illustrated in Figure 14.

It can be seen on the pot that there is metal added around where the legs are attached to the pot body, probably in an attempt to prevent them from breaking off. However, this was not sufficient enough, as the pots still are experiencing failure. To see if a geometry alteration could decrease the stresses along the leg of the pot, a new model was created and FEA

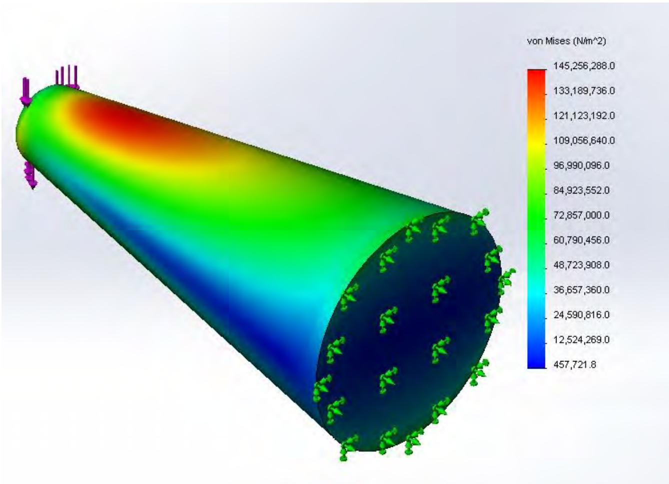

Fig. 15. This is a possible redesign of the leg of the pot. The maximum stress experienced here is 145 MPa, and since this is closer to the yield strength of aluminum, 192 MPa [12], a drop in this orientation probably would not cause fracture. If the pot was malleable or ductile cast iron, with a yield strength in the range of 224 MPa-864 MPa [14], it would not have experienced failure.

was performed. From these FEA results, again, when the leg was made out of aluminum, it was expected to fail, while when it was made out of iron, it was not. It is possible to conclude that a main factor the fracture of these pots is the material choice; in choosing aluminum over iron, it makes the pot a lot more susceptible to failure upon impact.

XI. Environmental Effects

The environmental effects of sand cast aluminum can be analyzed from several different angles: the recyclability of aluminum, the use of sand casting in place of casting methods that are more environmentally damaging, and the benefits of small scale sand casting over sand casting done on a large scale.

The compositional analysis suggests that the levels of the contaminants in the aluminum were not significant enough to be the main cause of brittle failure in the pot. Though there is no set method of collecting and recycling aluminum in Zambia, the composition of the pot suggests that this is not problematic. It would be environmentally beneficial to continue reusing aluminum in this way. Recycled aluminum uses only 5% of the energy that is needed to produce the metal from raw materials, which lends to a 95% decrease in greenhouses gases [5].

Sand casting has its environmental benefits over alternative casting methods. It uses only around two thirds the energy of other methods, such as die casting [6]. In die casting, molten metals are forced under high pressure into a mold of steel dies. An energy comparison between the two casting methods can be seen in Figure 16 [6][7]. It can be seen that Die Casting has a much higher proportion of energy in the casting and mold prep stages.

Small scale sand casting has benefits over sand casting done on a large scale. The sand casting techniques in Zambia are beneficial because clay is used as a binder and no chemical

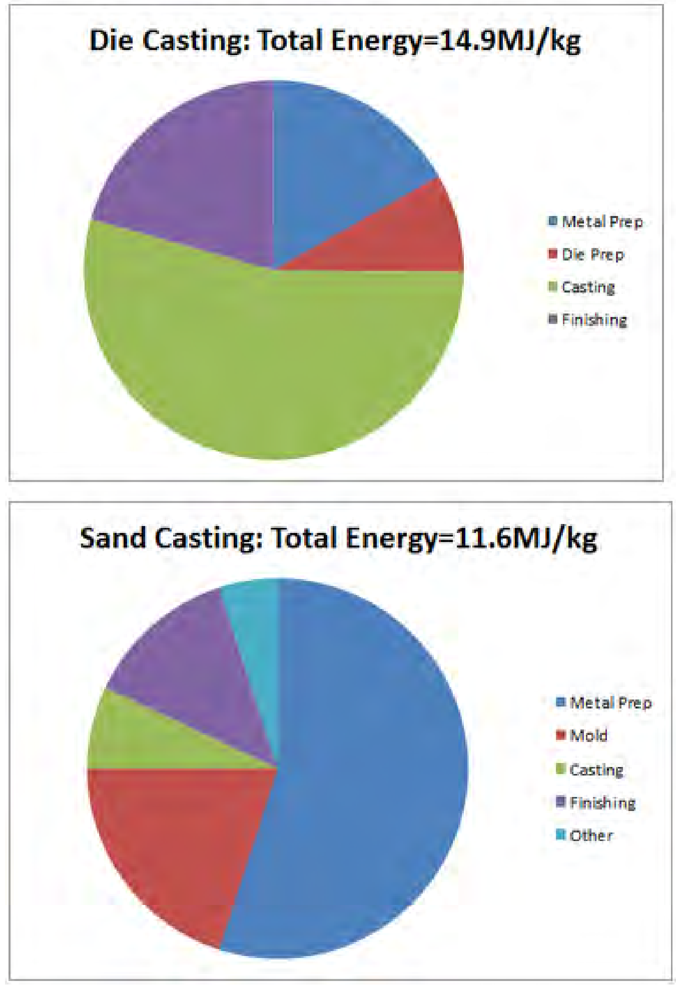

Fig. 16. A comparison of the environmental impact of sand and die casting

additives are used. When sand is chemically bound, the mold preparation stage uses three times the energy than when the sand is bound by clay. In addition, chemically binding sand releases pollutants such as benzene, methanol, phenol, toluene, and formaldehyde [7]. The relative quantities of these can be seen in Figure 17. There should be further analysis conducted on casting techniques to see if the defects from sand casting increase the pot's susceptibility to fracture. However, it is environmentally beneficial if this casting process can be continued without the use of chemical binders.

XII. Discussions and Suggestions

The compositional analyses that were conducted revealed that the recycled aluminum-silicon alloy that is being used to make these pots is not the main reason for the brittle fracture that many of these pots experience when dropped. The alloy does not have significant impurities. Rather, the main problem most likely lies in the fact that these pots were probably originally designed to be made out of iron, and are now being made out of aluminum. Though casting defects might play

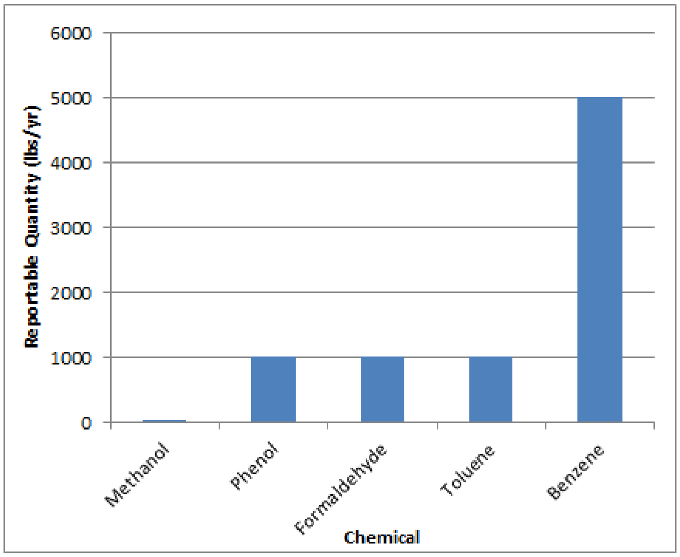

Fig. 17. Reported quantities of major pollutants

a role in premature fracture, the effects of these seem to be minimal, since there are minimal bubble inclusions, and visually, the surface finish does not have any major defects.

The main suggestion that could be given to the casters in Zambia is that in order to reduce the rate of failure of these pots the geometry of the legs should be altered. If the option is available, it would also be beneficial to revert to iron casting. The continuation of using recycled resources is not problematic, as there were minimal impurities seen in the cast aluminum.

XIII. Future Work

For future work on this project, a direct comparison of the material properties of the pot via machining a dog bone out of it and comparing it to a dog bone of a known commercial Al alloy would verify that casting techniques are not the source of the problem. To test the effects that surface defects that sand casting produces, sand cast dog bones and wax cast dog bones of the same size could be analyzed and compared. It would be interesting to do another experiment that compared the hypereutectic and hypoeutectic aluminum-iron alloys with larger dog bones to see if there are noticeable differences, since the results that were obtained in this project were obscured by relative size of air bubbles to cross sectional area that was being tested. Lastly, by working directly with casters to see what alternative ways that they can manufacture the legs, it would be useful to see what geometry works best to reduce the stresses along the legs.

Acknowledgments

The authors would like to thank Professors Jon Stolk, Matt Neal, and Ben Linder for providing us with the project idea, giving us advice, and helping us set up tests.

References

[1] Bank of Zambia, ”Zambia GDP annual growth rate” 2012.

[2] Personal Conversation with Professor Ben Linder.

[3] J. A. Taylor, ”The effect of iron in Al-Si casting alloys”, Cooperative Research Centre for Cast Metals Manufacturing, The University of Queensland, 2000.

[4] Rahavan, V. (2002). ”Al-Fe-Si (aluminum iron silicon)”, Journal of Phase Equilibria, 23(4), 362-366.

[5] J. Ratcliffe, ”Aluminum and sustainability: a ’cradle to cradle approach’”, The Council for Aluminum in Building, July 2008.

[6] S. Dalquist and T. Gutowski, ”Life cycle analysis of conventional manufacturing techniques: die casting”, LMP Working Paper, December 2004.

[7] Dalquist, Stephanie and Gutowski, Timothy, ”Life cycle analysis of conventional manufacturing techniques: sand casting”, 2004 ASME International Mechanical Engineering Congress & Exposition, November 2004.

[8] M. Stark, A tale of two tongs: the brittle truth of an alloy gone wrong, Olin College: Failure Analysis & Prevention, Fall 2010.

[9] J.L. Murray, A.J. McAllister Bull. Alloy Phase Diagrams, 5 (1984), p. 74.

[10] J. A. Taylor, ”The effect of iron in Al-Si casting alloys”, Cooperative Research Centre for Cast Metals Manufacturing, The University of Queensland, 2000.

[11] Traditional Cast Iron Pots from Africa. www.africantradingco.com/castironpots-info.html

[12] MatWeb Material Property Data, ”Aluminum 332.0-T5, Permanent Mold Cast”, .matweb.com/search/datasheet.aspx?matguid=7648a91e1a6c466791cd69fc82773ae1&ckck=1

[13] J. P. Byers, ”Metalworking Fluids, Second Edition”, CRC Press, 2012.

[14] McGraw-Hill, ”Materials Properties Database”, http://highered.mcgraw-hill.com/sites/dl/free/007253586/240416/Materials_Properties_Database.xls